Mads O'Brien
Prof. Xuhui Lee
Remote Sensing & Photogrammetry
18 December 2018

Estimating Volume Changes in Volcanic Features with UAV Photogrammetry

1) Introduction and Setting

After decades of dormancy, Mount Kilauea on the Big Island of Hawai'i began actively erupting on May 3, 2018. In addition to lava fountaining and crater collapse at the Kilauea summit, twenty-four volcanic fissures opened in a mostly-developed area of the eastern island known as the East Rift Zone *[Figure 1]*. The eruption and its damages gained extensive media and scientific attention.

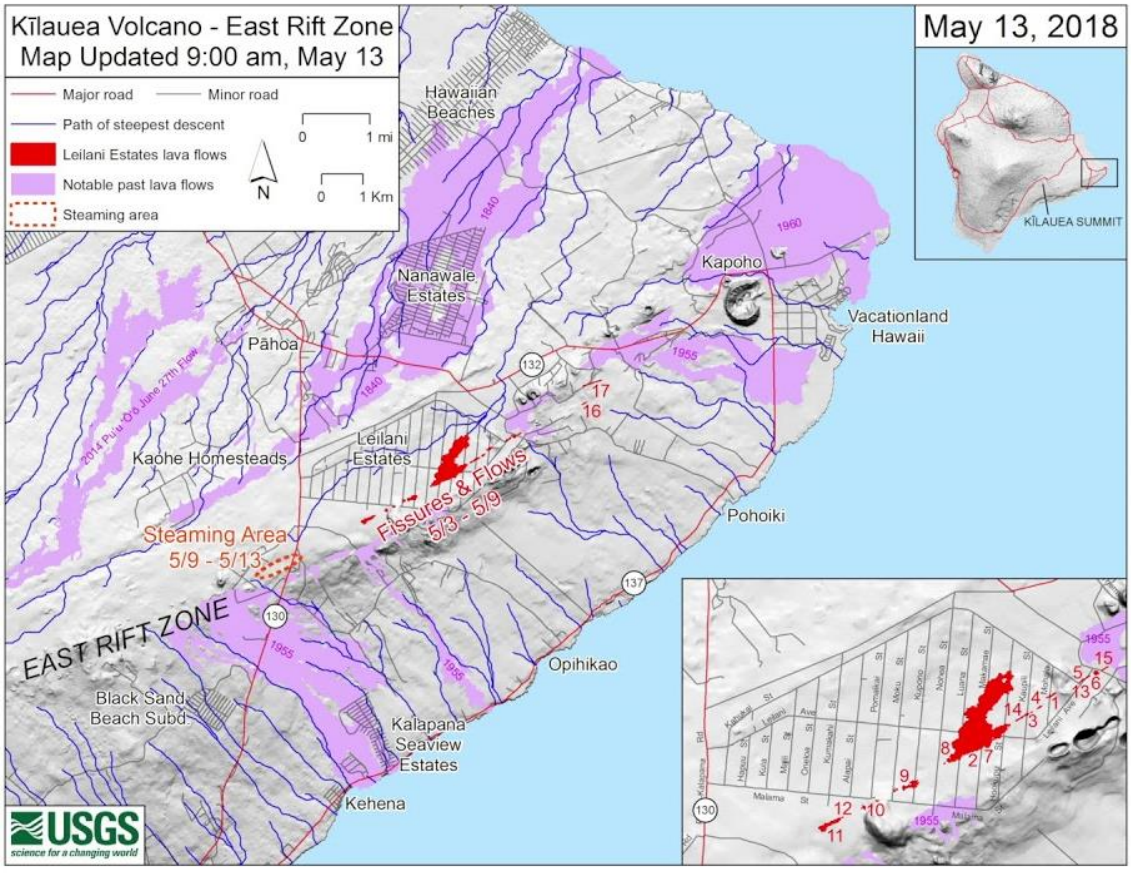

Figure 1: Map of the East Rift Zone in Hawai'i showing eruption extent on May 13 2018. Inset map shows location of F8 in Leilani Estates. [Source: USGS]

It is vital that scientists monitor volcanic features during and immediately after activity to assess what danger they pose to the public. However, collecting data close to such features is dangerous itself. Remote volcano monitoring carries huge potential for

(a) assessing danger from a distance and (b) creating virtual models of features that help scientists study their structure and behavior.

Of the 24 fissures, Fissure #8 (F8), which appeared May 3 in the Leilani Estates subdivision, has been the most active and most closely observed fissure during this eruption phase. F8 is a ground crack that has developed a “spatter cone” due to fountaining lava falling back to the ground beside the crack *[Figure 2]*. The feature is characterized by its size and its dynamic rate of change: daily U.S. Geological Survey (USGS) monitoring logs indicate that F8 endures long periods without activity, but in heavy lava fountain conditions has grown from 115 ft to 170 ft (35.1 to 51.8 m) over six days (6/11-6/16) (U.S. Geological Survey, 2018). The feature currently stands at 180 ft. (54.9 m) tall. F8 and the Eastern Rift Zone are thought to have entered a “paused” eruption phase, but F8 continues to exhibit weak signs of lava activity and could become violently active again at any time (U.S. Geological Survey, 2018).

Figure 2: Lava flowing from F8 on June 20, 2018. Note trees in background for scale. [Source: USGS]

F8 is a prime candidate for observation by an unmanned aerial vehicle (UAV) because its features are too small to discern from satellite imagery and its change is much more dynamic than the return time of most satellites.

2) Project Objectives

1. Create a 3D mesh model and digital elevation model (DEM) of the F8 spatter cone and lava channel using imagery from two UAV flights, seven days apart
2. Georeference a 3D model of F8 whose input images lack GPS coordinates

3. Calculate the volume of differences in the F8 cone between both acquisition dates
4. Assess the height and terrain of the F8 cone in the UAV-derived models, relative to a LIDAR-derived surface measured earlier in Summer 2018
5. Create cross-sections of F8 from all dates to visualize and quantify changes

3) Data Description

Drone imagery of F8 was acquired by USGS field personnel seven days apart, on August 27 and September 2 of 2018. The specifications of those flights are described in the table below. Images were not radiometrically corrected or exposure adjusted before analysis because this work did not require the comparison of specific reflectance values over time.

	27-Aug	**2-Sep**
Drone model	DJI Matrice 600 Hexacopter	
Camera model	Ricoh Imaging Co. GR II	
Flight area	~ 8 hectares (0.08 km^2)	
Coordinate system & projection	WGS 84, UTM Zone 5N (GRS1980 ellipsoid)	
Num. of images	58, 87 (145 total)	209
Focal length	5mm	18mm
Flight time(s)	1:51-1:59pm; 2:22-2:30pm	2:59pm-3:06pm
Image size (pixels)	4000x3000	4928x3264
Geolocation	Bad Elf Surveyor GPS, no ground control points	No GPS or ground control points
Flight pattern	Radial around feature (some oblique)	Grid (orthogonal to ground)

To compare the Aug 27 and Sept 2 models of F8 to an earlier stage of the eruption, a LIDAR-derived DEM was acquired. The LIDAR was flown July 8 – July 12, 2018, by USGS and collaborators, and the data are free to download from OpenTopography.com. The LIDAR-derived DEM has a pixel resolution of 0.5 m and includes some NoData masks in and around F8. All spatial data were re-projected into the NAD 1983 (PA11), UTM Zone 5N coordinate system for consistency.

4) Methods

All point clouds, DEMs, and orthophoto mosaics were constructed in AgiSoft Photoscan Pro 1.3.2. Methods for creating these products can be found in tutorial workflows published by AgiSoft (Agisoft, n.d.). Any minor deviations from those instructions are noted in this manuscript. DEMs were then exported to ArcMap 10.6 for height calculations and digitization of features. 3D image rendering and volume calculations were conducted in ArcScene 10.6.

3D Model and DEM Creation

Photo alignment, alignment optimization, point cloud construction, DEM construction, and orthomosaicking were conducted using Agisoft’s published workflow (Agisoft, n.d.). For the Aug 27 images, camera positions were auto-loaded from photo EXIF data. When constructing the dense cloud for both models, “moderate” depth filtering was used as opposed to “aggressive” to retain small, complex ground features. DEMs were constructed from the dense point cloud rather than 3D mesh to ensure finer resolution terrain. Additional points were manually deleted from the Aug 27 model that appeared to be noise, such as those projecting far beneath the terrain surface or floating high above the features. Color was also used to discern erroneous points; for example, bright white points were suspected to derive from steam in the images. The Sept 2 model did not require significant pixel deletion.

Georeferencing the Sept 2 3D model

Because no ground control points (GCPs) have been surveyed in the F8 region, field-truthed GPS coordinates cannot be assigned to either models. However, the Aug 27 images were recorded with associated GPS coordinates, and the resulting model is automatically assigned reference information in Photoscan. Since the Sept 2 flight did not record image location, the orthomosaic generated from the Aug 27 flight was treated as a “remote ground truth” for georeferencing the Sept 2 images.

The Aug 27 orthomosaic was inspected for 20 distinct features that also appeared in the Sept 2 imagery with good distribution across the scene. Shapefile points were placed on the orthomosaic in ArcMap 10.6, and the northing, easting, and altitude of each point was extracted from the corresponding Aug 27 DEM and stored in a value table. Point placement was conducted at a zoom level of 1:200 map scale or closer to ensure accuracy. Point placement on steep slopes (i.e. areas with large height change over short distances) was avoided to decrease variability in elevation recording. Points were also not placed within the lava moat or dome because these locations may have varied between exposure days. Next, following Agisoft’s workflow, “markers” were created within the Sept 2 point cloud and the coordinate table was imported to assign

each marker lat-long information *[Figure 3]*. Once georeferenced, the same steps as above were used (Agisoft, n.d.) to generate a dense point cloud, DEM, and orthomosaic for Sept 2.

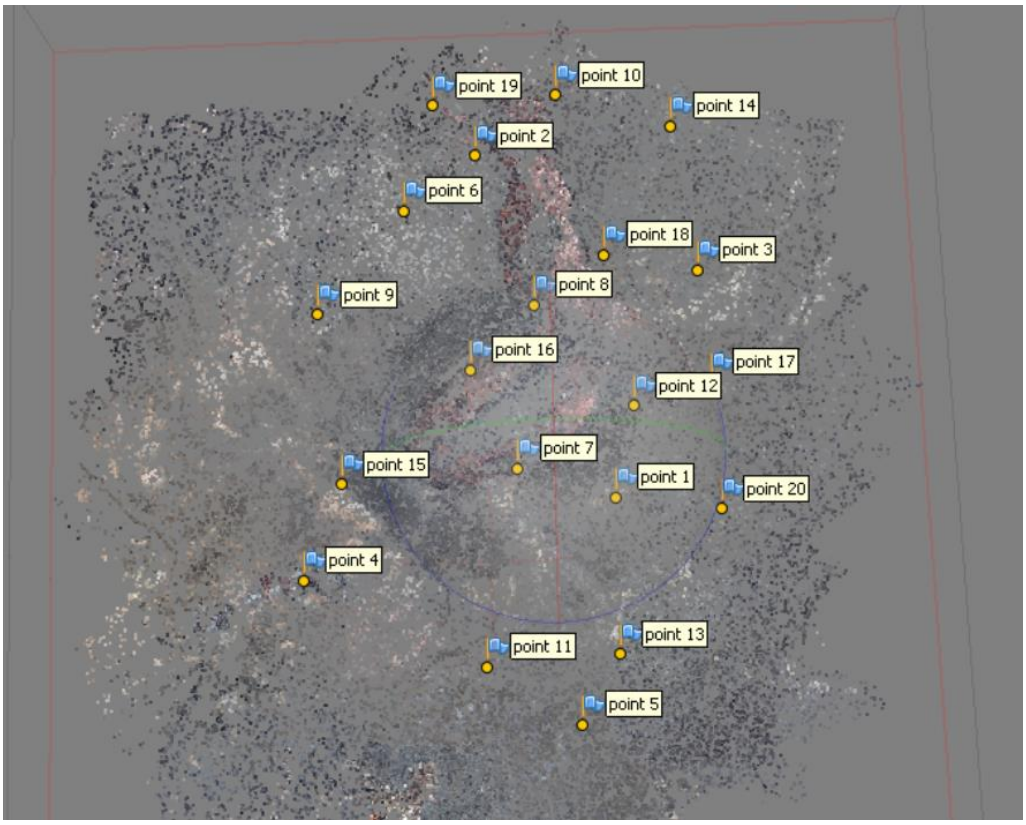

Figure 3: Markers used for georeferencing the Sept 2 point cloud (shown here) relative to the Aug 27 orthophoto.

Volumes of F8 on Aug 27 and Sept 2

The surfaces of the cone for both dates were compared by creating a difference surface (September minus August) using raster algebra. Contiguous regions of high vertical difference were digitized and clipped if they corresponded to changes in the orthophotos. The volumetric difference between the two surfaces within the clipped area was then calculated using the Cut Fill tool in ArcScene.

Model comparisons to LIDAR

Upon visual inspection, both UAV-derived elevation models appeared systematically lower than the LIDAR elevation model. Due to uncertainty about the proper vertical coordinate system for the UAV-based models, a conversion to the LIDAR coordinate system could not be conducted (see more in Interpretations). Instead, the average vertical difference between the LIDAR and each DEM raster surface was calculated with raster algebra. The resulting average value was added as a vertical shift to the Aug 27 and Sept 2 DEM to make each terrain more comparable to the LIDAR.

This shift was only utilized to generate comparative cross sections with the LIDAR terrain; elevation scales in the figures of this manuscript and in volume calculations reflect the original scales calculated from the DEMs. Lastly, slope maps were built from all three DEMs using ArcMap's Calculate Slope tool, to compare the morphology of the structures over time.

Cross sections of F8

Cross section lines were drawn in ArcMap across regions of potential surface change suggested by the analyses above *[Figure 4]*. Elevation profiles were generated for each line using the Stack Profile 3D Analyst tool in ArcMap, and profiles for July, August, and September were plotted simultaneously.

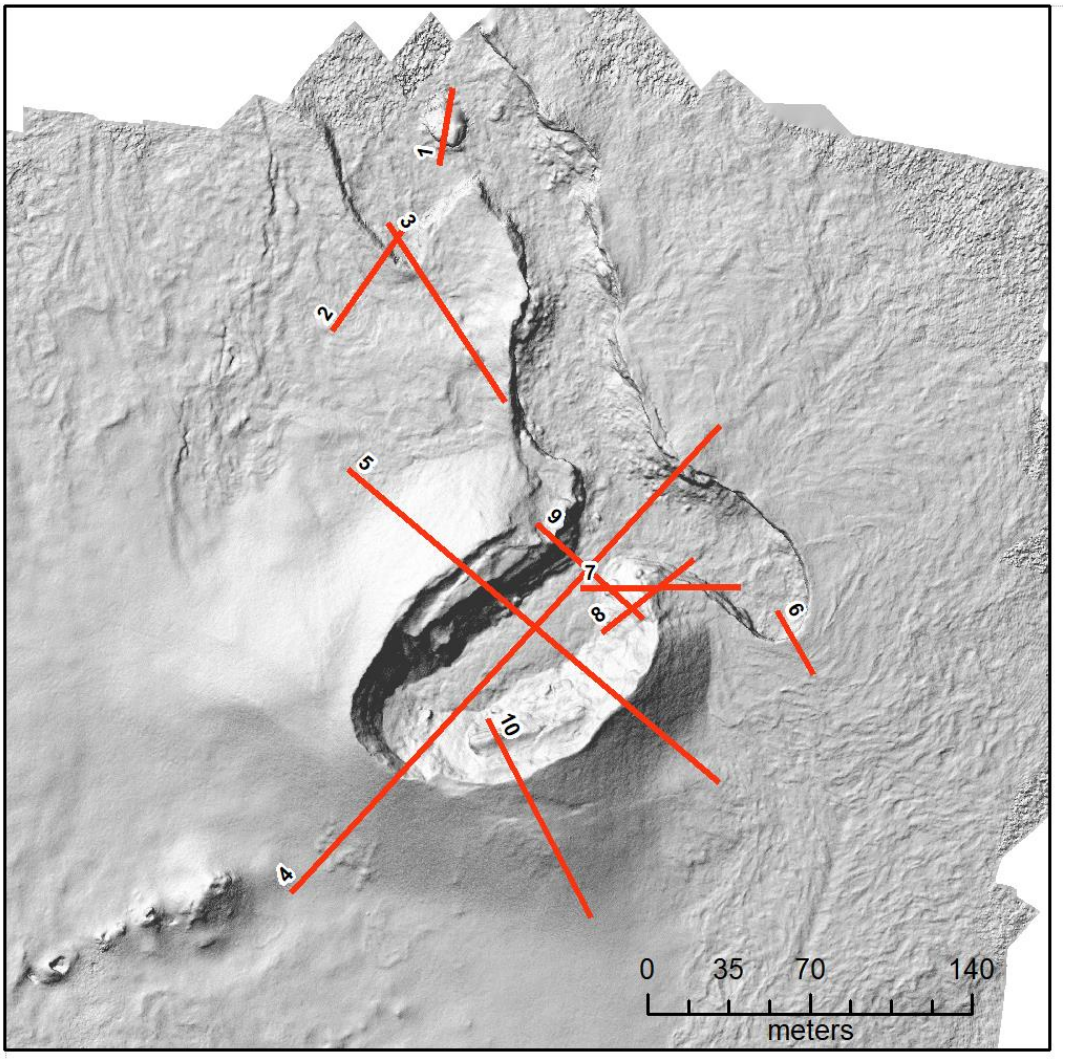

Figure 4: Location of cross section lines. Line ID numbers are placed at the "starting point" of each cross section.

5) Results

3D Model and DEM Creation

A table describing the quality of the processed models is below. All 145 of the Aug 27 images were automatically georeferenced, with an estimated horizontal error of 1.05 m and vertical error of 0.87 m.

Flight Date	**# of tie points**	**DEM resolution (cm/pix)**	**Orthophoto resolution (cm/pix)**
August 27	105,460	22.27	5.57
September 2	88,910	16.17	4.04

Both DEMs *[Figure 6]* depict a vertical range of about 41-44 m (134.5 – 144.3 ft) from the lowest point in the lava channel to the top of the cone. The Aug 27 DEM has a large amount of noise and highly interpolated surfaces along the southern cone rim and the area southwest (down-wind) of the cone. The DEM captures an adjacent fissure, F7, visible in the lower-left of the Sept 2 DEM, but the feature is harder to discern within the noise in the Aug 27 DEM.

Figure 5: An oblique view of the Sept 2 3D model, looking northwest.

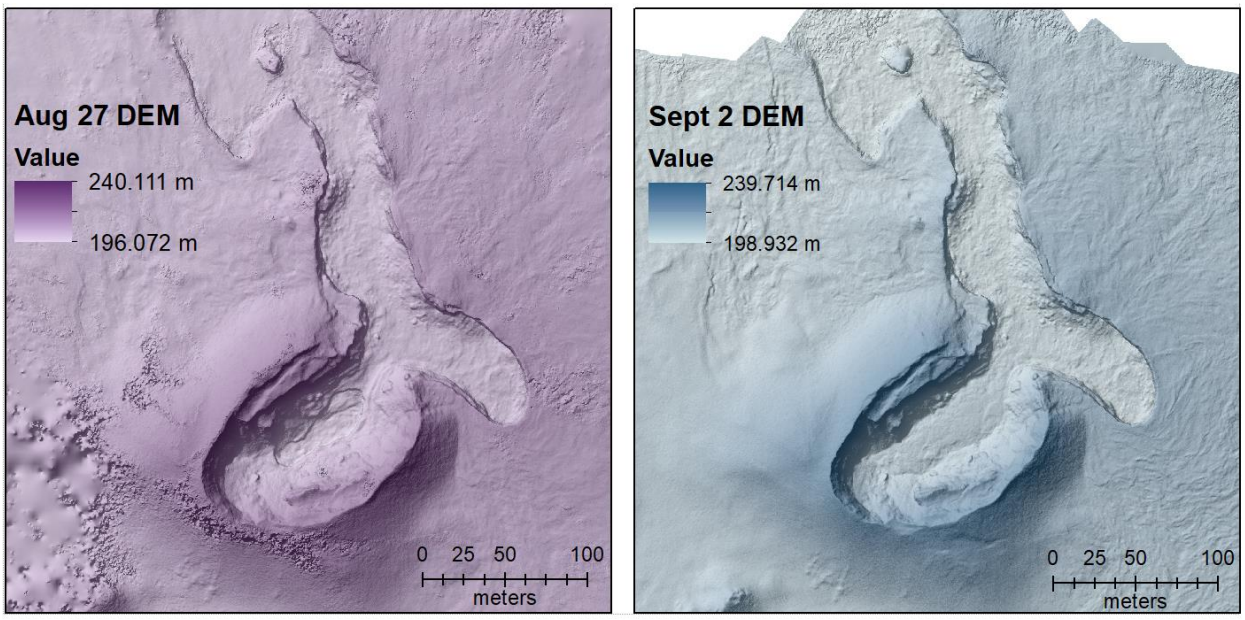

Figure 6: UAV-derived DEMs with a hillshade applied to express terrain. Elevations are in meters above mean sea level.

Georeferencing Sept 2 3D model

Visually, the Sept 2 model aligned very well with the Aug 27 model in geographic space. The Sept 2 point cloud aligned to the 20 photo-based control points with a total horizontal error of 0.18 m and vertical error of 0.16 m according to Photoscan.

A difference raster was also calculated between the two surfaces (Aug 27 minus Sept 2) to quantify vertical differences between them. The two surfaces vertically differ approximately +0.23 m (1.37 m stdev), with a minimum difference of -21.83 m and a maximum difference of +25.89 m. This result suggests that on average, the Sept 2 surface is lower than the Aug 27 surface. However, the average is likely skewed by (a) the noise in the Aug 27 surface and (b) zones of extreme vertical difference caused by horizontal misalignment between the Sept 2 and Aug 27 DEMs.

Volumes of F8 on Aug 27 and Sept 2

While the volume differences between the two models are negligible in most places, the zone of greatest volume difference lies in the center of the cone, where an elevated surface of what appears to be new lava is seen in the Sept 2 model *[Figure 7, Figure 8]*. The new lava pool covers 2,609 m^2 and its volume is 13,066 m^3. Because the area of the outlined feature differs -0.002% when calculated as a raster vs. a shapefile, one can assign this margin of error to the volume estimate as well (±28.09 m^3).

Figure 7: Aug 27 orthophoto (left) and Sept 2 orthophoto (right). The region of new lava is outlined in yellow. The area of the new lava on Sept 2 was digitized by hand at 1:50 map scale.

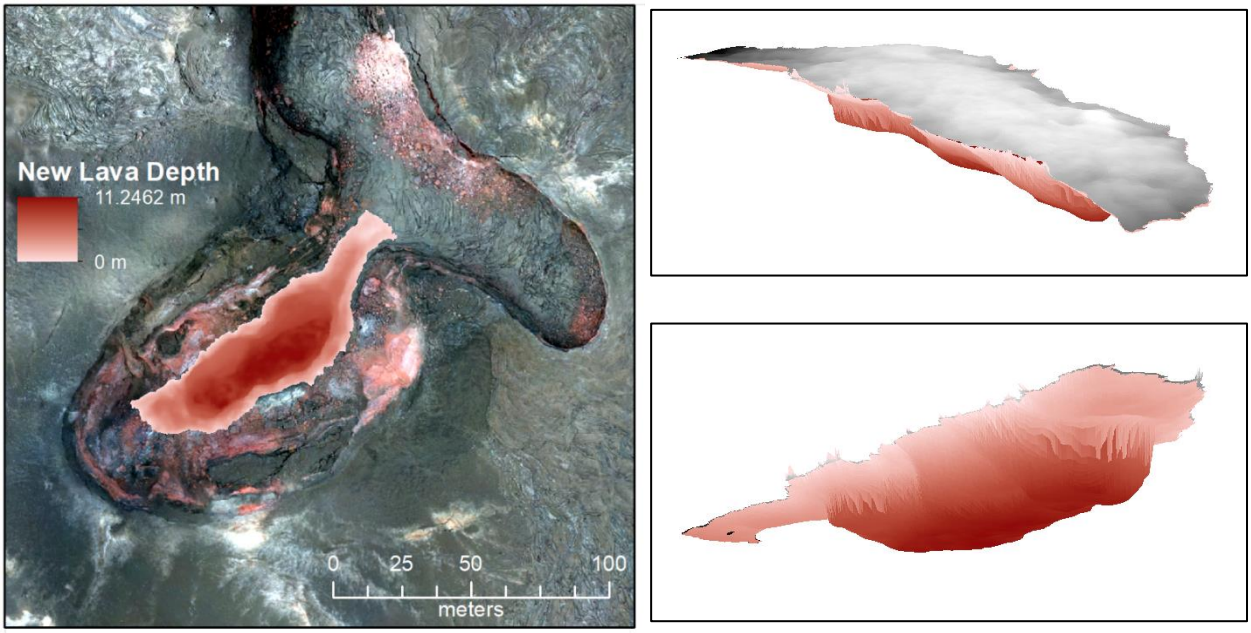

Figure 8. New lava feature symbolized according to depth, superimposed on Sept 2 orthophoto (left). 3D rendering of the lava structure, from above (top right) and below (bottom right).

Model comparisons to LIDAR

The elevations generated for both UAV DEMs are systematically lower than the July LIDAR-derived elevations. A difference raster between the UAV and LIDAR DEMs *[Figure 9]* reveals that the Aug 27 DEM is on average 21.97 m lower than the July DEM, and the Sept 2 DEM is 22.79 m lower. Though the LIDAR's masks conceal much of the

cone interior in July, the image indicates there are slightly lower slopes on the inside walls of the cone during July compared to Sept 2, in addition to a narrower, steeper vein of lava in the channel *[Figure 10]*.

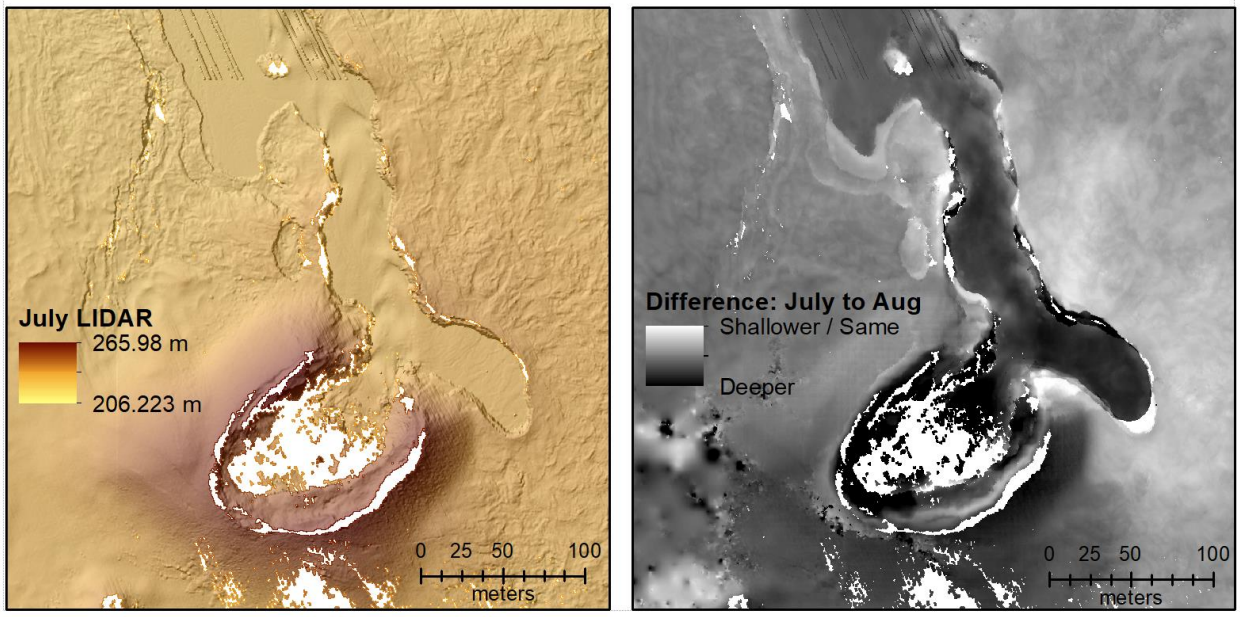

Figure 9. DEM derived from July LIDAR (left) and difference raster between the July and Aug 27 DEM (right). Light areas in the difference image indicate areas of stasis or growth from July to August, while darker areas indicate recession.

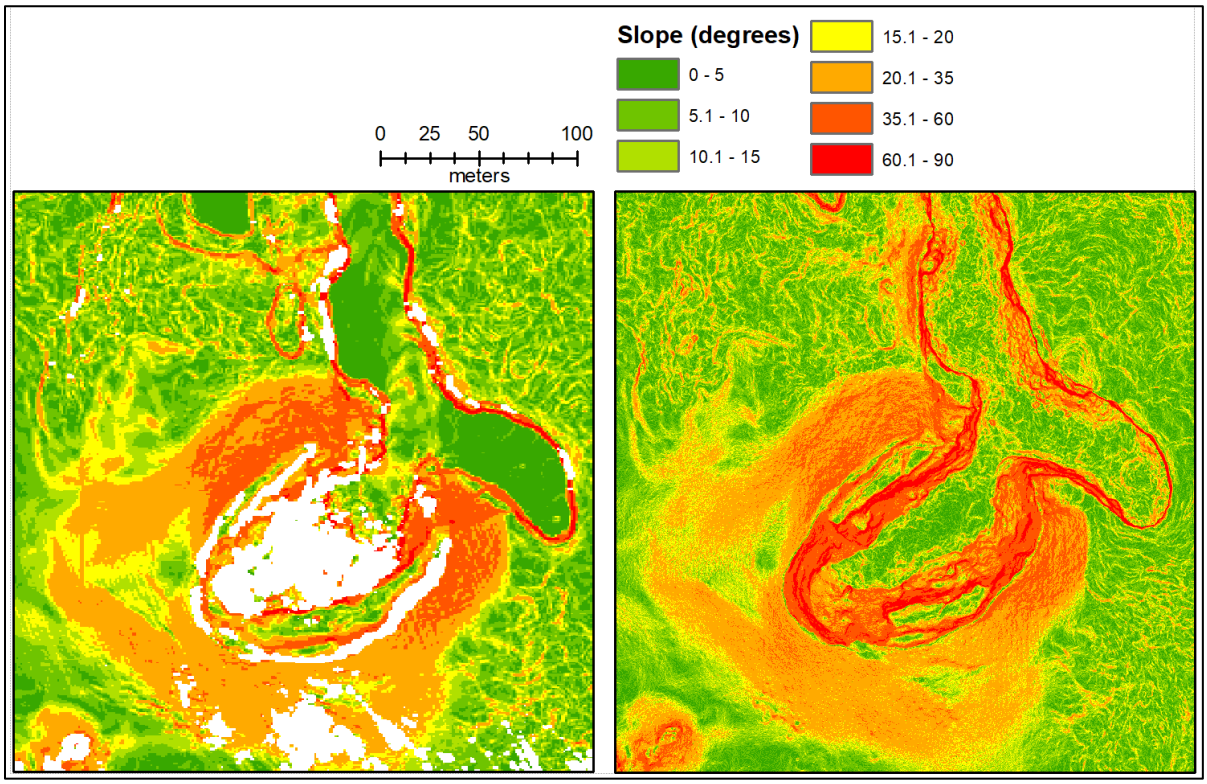

Figure 10: Slope map of F8 based on July LIDAR (left) and Sept 2 modeled DEM (right). White pixels in the July image are NoData values.

Cross sections of F8

All ten cross-sections illustrate strong agreement between the Aug 27 and Sept 2 terrain. Many of these profiles exhibit greater vertical exaggeration than what appear to be the same features in the July LIDAR profiles. (See Appendix for all profiles.)

6) Interpretations

Model creation and accuracy

On-the-ground F8 monitoring reports were searched to find similarities between the 3D models and the fissure on UAV flight dates. Observations state that on September 1, the crater floor measured 65 by 15 m (210 by 45 ft) (Volcano Science Center, 2018). Bisecting measurements in the Aug 27 orthophoto indicate the lowest inner crater surface is 65.8 m and 15.2 m. This finding strongly supports that the model is functionally accurate for quantifying horizontal structural changes. Meanwhile, vertical accuracy is less certain. The Aug 27 3D model and DEM display significant surface noise due to excessive volcanic steam in the UAV photos. Though some tie points were removed manually based on erroneous color and elevation, this process was not comprehensive and not particularly reproducible. Automated point filtering methods would greatly improve DEM construction from point clouds.

Volumes of features

The crater volume increase between August and September found in this study is corroborated by USGS reports of a "weakly active" lava lake in early September (Volcano Science Center, 2018). Indeed, in the Sept 2 orthophoto, two holes in the hardened lava surface reveal incandescent fresh lava beneath. The brighter color of the hardened lava also indicates its freshness.

September 1 observation reports indicate that emerging lava covered the crater floor by that evening (Volcano Science Center, 2018). If one assumes the early morning of September 1 as the start date of lava extrusion, then lava filled the crater to the size calculated in this study in roughly a day and a half (~36 hours) since the Sept 2 imagery was taken around 3pm. This corresponds to a ballpark pooling rate of 363 m^3 per hour.

Model comparisons to LIDAR

Dramatic vertical differences (as high as 14 m) reported between July and August along the edges of the lava channel are most likely due to horizontal misalignment of the LIDAR and UAV models, causing the edges of steep slopes to become offset. Manual horizontal measurements suggest that the UAV DEMs are displaced 5-6 m to the southeast relative to the LIDAR surface. This horizontal

displacement is likely a product of horizontal inaccuracies in the Aug 27 GPS readings on the UAV, since they were not adjusted with GCPs.

Systematic vertical difference between the LIDAR and UAV-based models may arise from a disagreement between the geoid model used to calculate the LIDAR base heights (GEOID09) and the drone GPS altitudes based on reference to an ellipsoid (GRS 1980). Though attempts were made to convert UAV ellipsoid-based heights to geoid-based heights in Photoscan, the conversion failed for unknown reasons. Interestingly, other work has found that difference between mean sea level (geoid) height and ellipsoid-based height is only 0.51 meters on average in Hawai’i (Waters, 2018), dramatically smaller than the difference found here. If Waters’s finding is true, another factor must be responsible for the dramatic vertical offset of the UAV data, such as problems with the onboard GPS. Since significant issues impede proper vertical alignment of UAV models and the July DEM, differences between the two are discussed qualitatively below.

Two zones of significant channel shallowing between July and August *[Figure 11]* are much wider than the 5-6 m horizontal error identified between the two DEMs. This suggests that these zones may represent actual changes in lava channel morphology. One possible explanation is that slow-moving lava built up in the bends of the channel, much like sediment will deposit in river bends. When the lava channel is very full, slow-moving overflows will further build up the levees on the side of the channel (Volcano Science Center, 2018). The identification of these locations as zones where slow-moving lava may pool may have implications for future work modeling the flow dynamics of the lava.

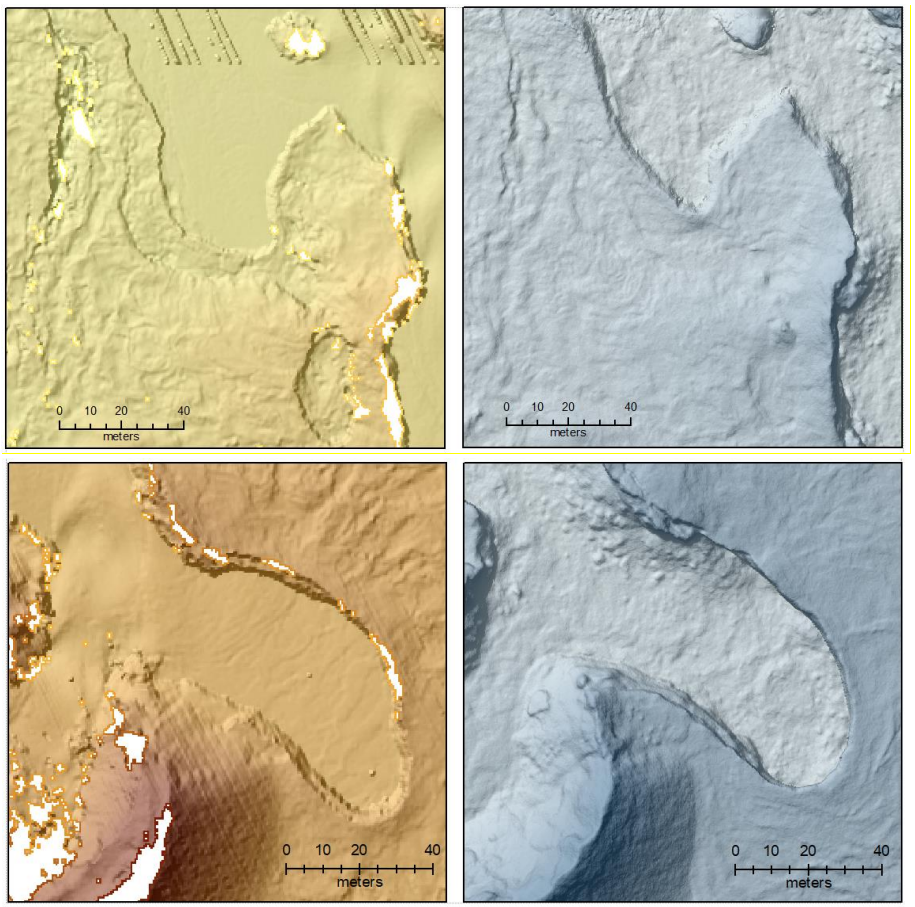

Figure 11: Areas of apparent growth or lava accumulation between July and September 2018.

Cross sections of F8

The elevation gains in Profiles 4, 5, and 9 are consistent with the measured height of the lava lake within the F8 crater. Profiles 4 and 5 show a distinct inflation in the center of the cone between Aug and Sept, with Profile 9 showing a slight height gain at the “mouth” of the lava channel. Additionally, Profiles 4, 5, and 8 exhibit evidence that lava level flowing out of F8 was higher on the day of the LIDAR—approximately 15-20 m higher, if one treats the base of the Aug 27 crater as the crater floor. This finding agrees with ground crew observations of steady lava eruption into the channel between July 8-12 (Volcano Science Center, 2018). Other areas of F8 are less dynamic than the orthophotos or DEMs suggest. Despite the horizontal offset, Profile 10 suggests that the elongate rock feature within the cone has not changed between July and September.

7) Limitations and Conclusions

- Lava lake appeared sometime between Aug 27 and Sept 2 amounting to 13,066 m^3 (±28.09 m^3). Under the assumption of lava infill starting on Sept 1, estimated rate of lava fill is 363 m^3 per hour.
- Two zones of significant channel shallowing developed between July and August 27, likely due to pooling slow-moving lava hardening into basalt rock.
- The area of the crater floor as of September 1 matches the size of the crater floor in the Aug 27 flight almost exactly, affirming that UAV imagery flown with these parameters are effective for producing useful models for earth scientists.
- Due to potential base height incompatibilities, differences between UAV models and LIDAR elevation models can only be assessed qualitatively. However, model cross sections corroborate field observations that the lava channel was very full during the days of the LIDAR collection, approximately 15-20 m higher than its level during September 2.
- Georeferencing a 3D point cloud of a geologic feature to an earlier orthomosaic allows successful measurement of change detection in the feature when lacking GCPs. Twenty control points are sufficient for successful alignment, assuming points are placed on flat areas that do not change.
- Future work of this nature should find better ways of dealing with steam. Solutions could include robust, reproducible filters to remove steam-generated noisy points from the point cloud, or simply masking steamy areas as NoData before analysis.

References:

Agisoft. "Orthophoto & DEM Generation (without GCPs)." *Support: Tutorials*, Agisoft, www.agisoft.com/support/tutorials/beginner-level/.

U.S. Geological Survey. "Kilauea Volcano Erupts." *USGS.gov*, U.S. Geological Survey, 21 June 2018, www.usgs.gov/news/k-lauea-volcano-erupts.

Volcano Science Center. *Kīlauea Volcano – 2018 Summit and Lower East Rift Zone (LERZ) Brief Overview of Events April 17 to October 5, 2018*. U.S. Geological Survey, 2018, *Kīlauea Volcano – 2018 Summit and Lower East Rift Zone (LERZ) Brief Overview of Events April 17 to October 5, 2018*, volcanoes.usgs.gov/vsc/file_mngr/file-179/Chronology of events 2018.pdf.

Waters, Kirk. "Vertical Datums in Paradise." *Digital Coast GeoZone*, 16 Mar. 2018, geozoneblog.wordpress.com/2018/03/15/vertical-datums-in-paradise/.

Data Sources:

USGS (2018b): Kilauea Volcano, HI July 2018 Acquisition airborne lidar survey. U.S. Geological Survey (USGS) in collaboration with the State of Hawaii, Federal Emergency Management Agency, Cold Regions Research and Engineering Laboratory, and the National Center for Airborne Laser Mapping, distributed by OpenTopography. https://doi.org/10.5069/G9M32SV1

Acknowledgements to Angie Dieffenbach, Cascades Volcano Observatory, US Geological Survey, for sharing this UAV imagery.

Appendix: Cross Section Graphs. X-axis = horizontal distance (m). Y-axis = ht. above mean sea level (m)

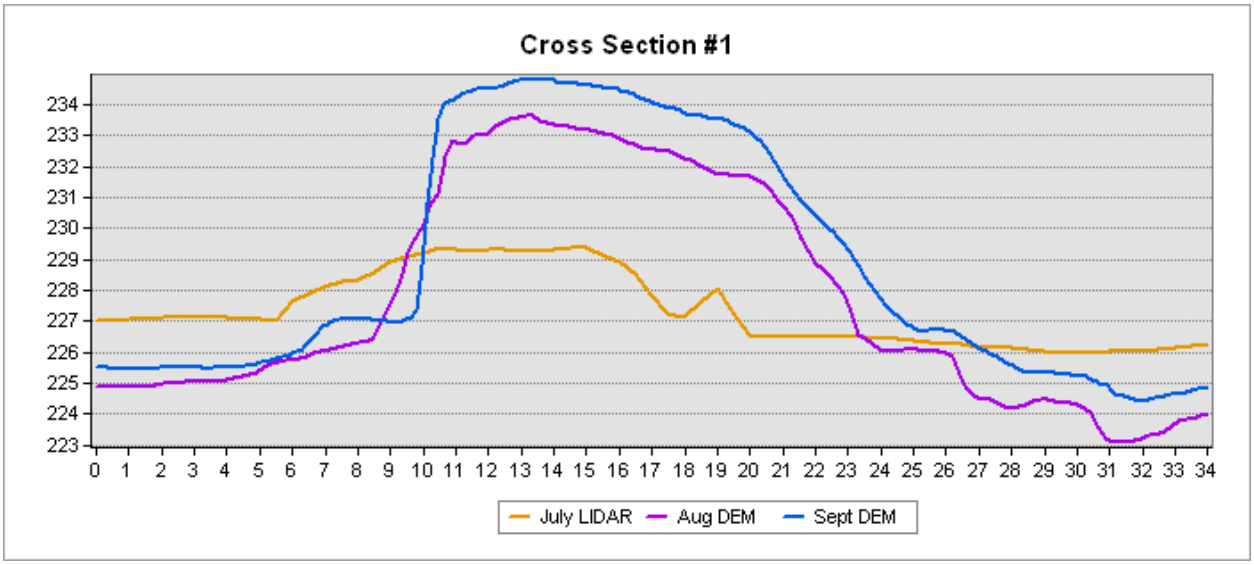

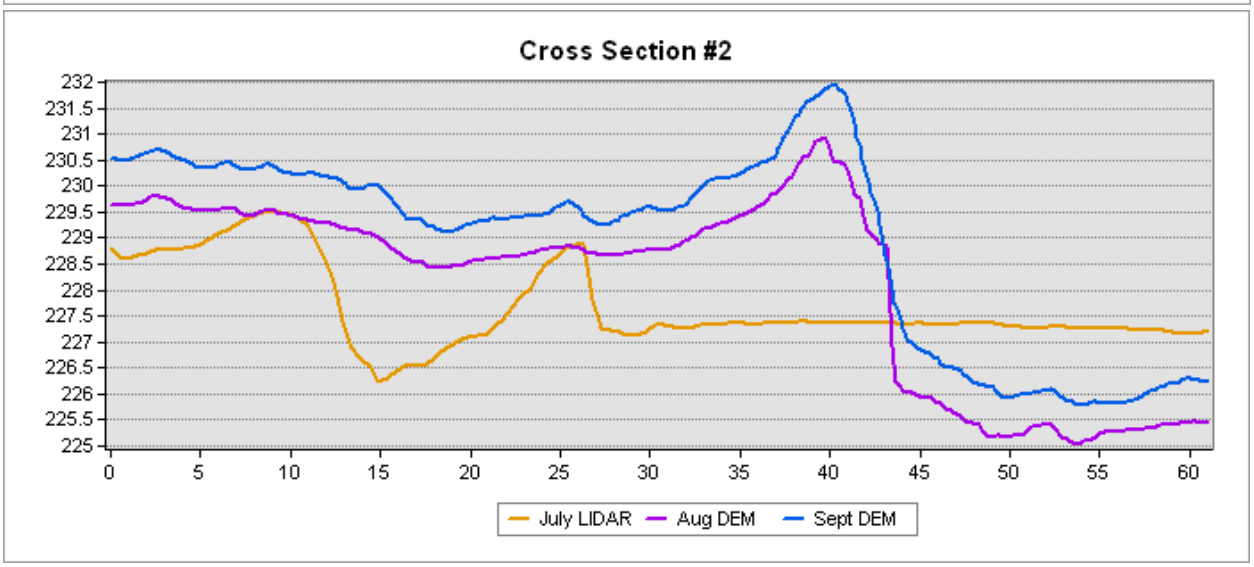

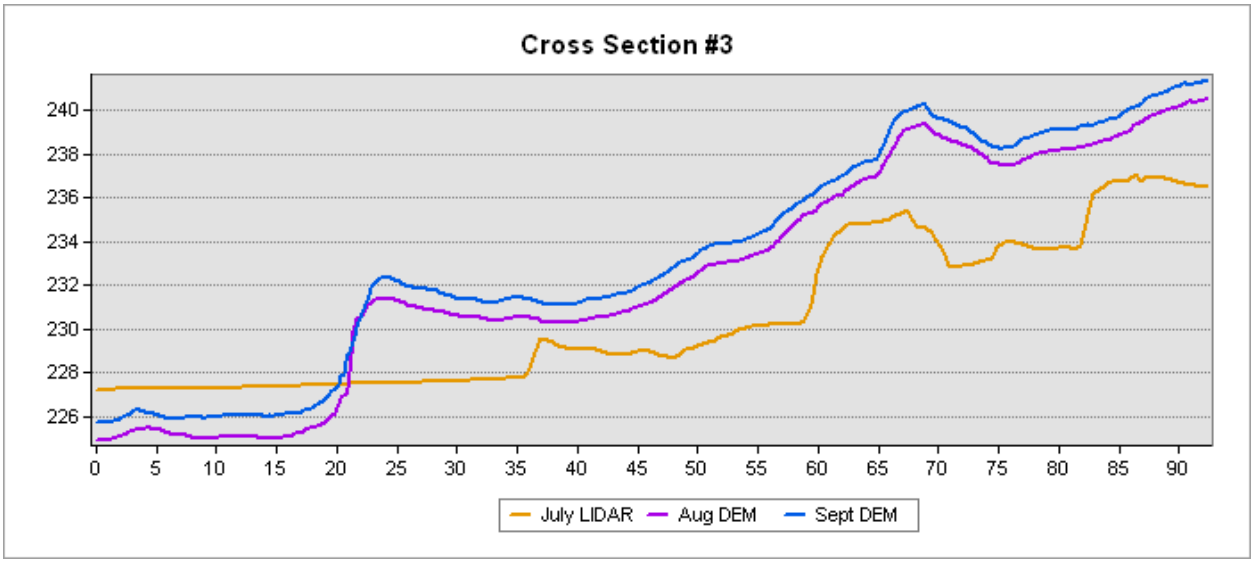

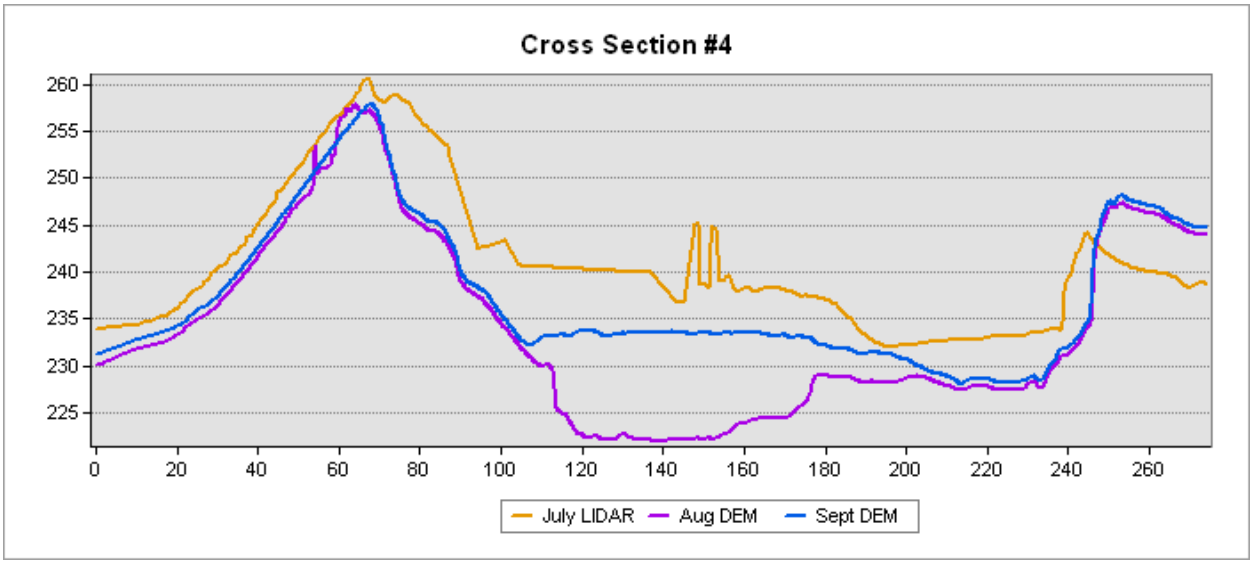
Cross Section #4
260
255
250
245
240
235
230
225
0 20 40 60 80 100 120 140 160 180 200 220 240 260
July LIDAR
Aug DEM
Sept DEM

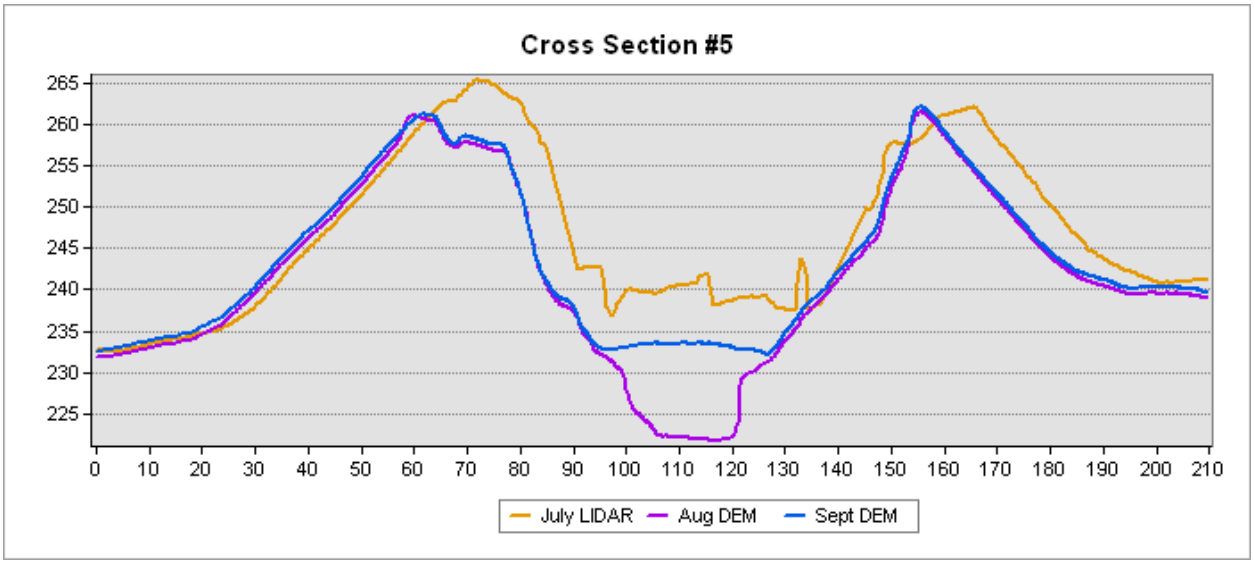
Cross Section #5
265
260
255
250
245
240
235
230
225
0 10 20 30 40 50 60 70 80 90 100 110 120 130 140 150 160 170 180 190 200 210
July LIDAR
Aug DEM
Sept DEM

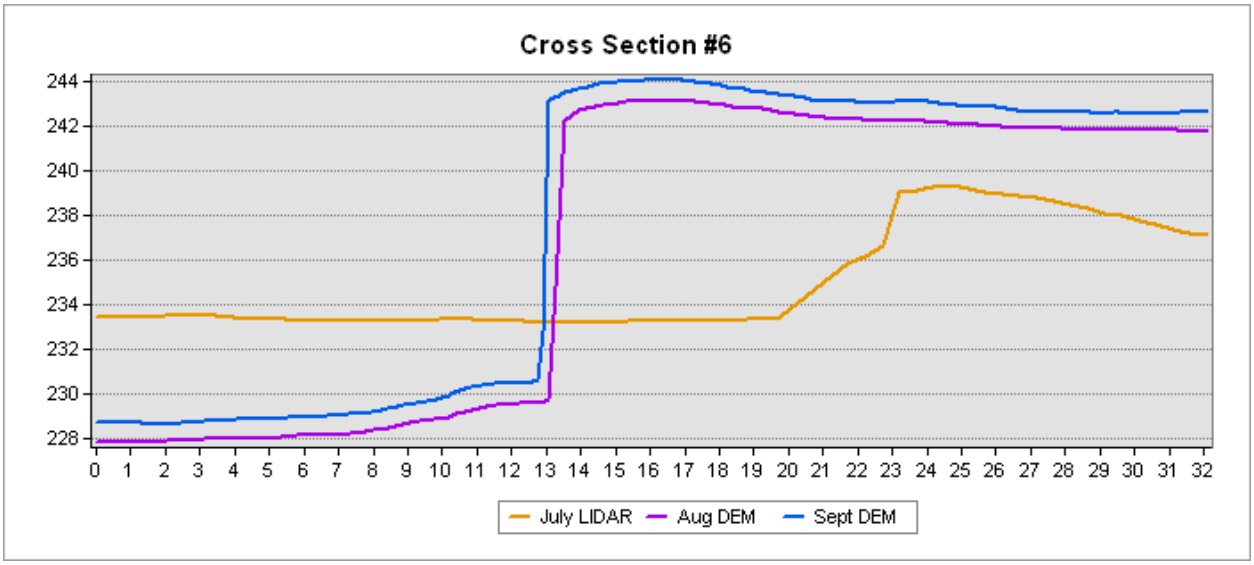
Cross Section #6
244
242
240
238
236
234
232
230
228
0 1 2 3 4 5 6 7 8 9 10 11 12 13 14 15 16 17 18 19 20 21 22 23 24 25 26 27 28 29 30 31 32
July LIDAR
Aug DEM
Sept DEM

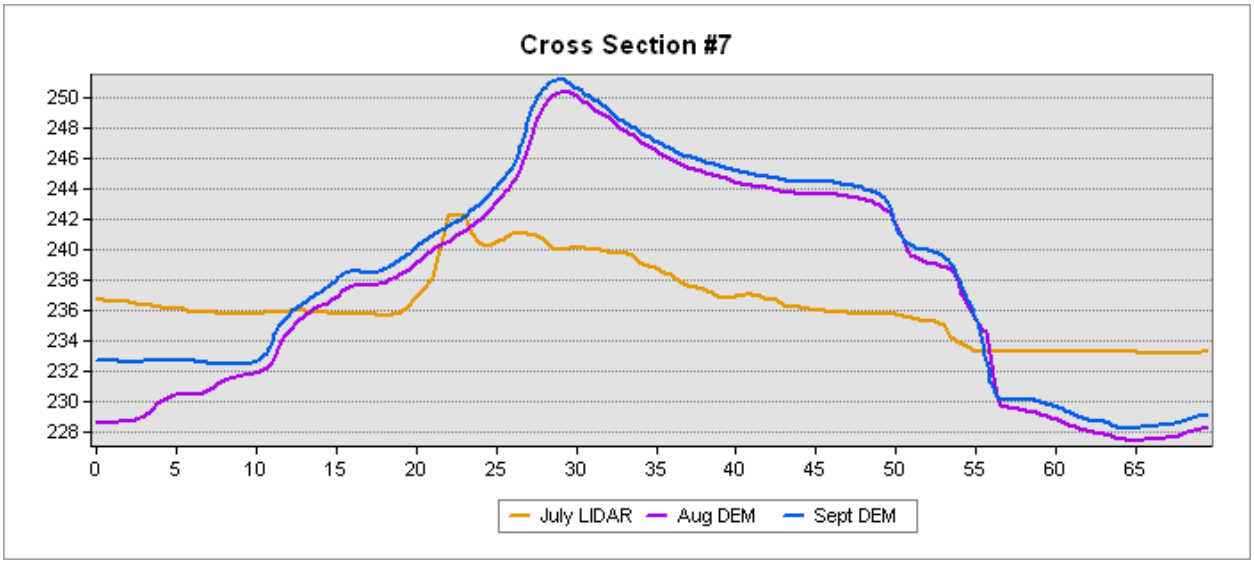
Cross Section #7
250
248
246
244
242
240
238
236
234
232
230
228
0
5
10
15
20
25
30
35
40
45
50
55
60
65
July LIDAR
Aug DEM
Sept DEM

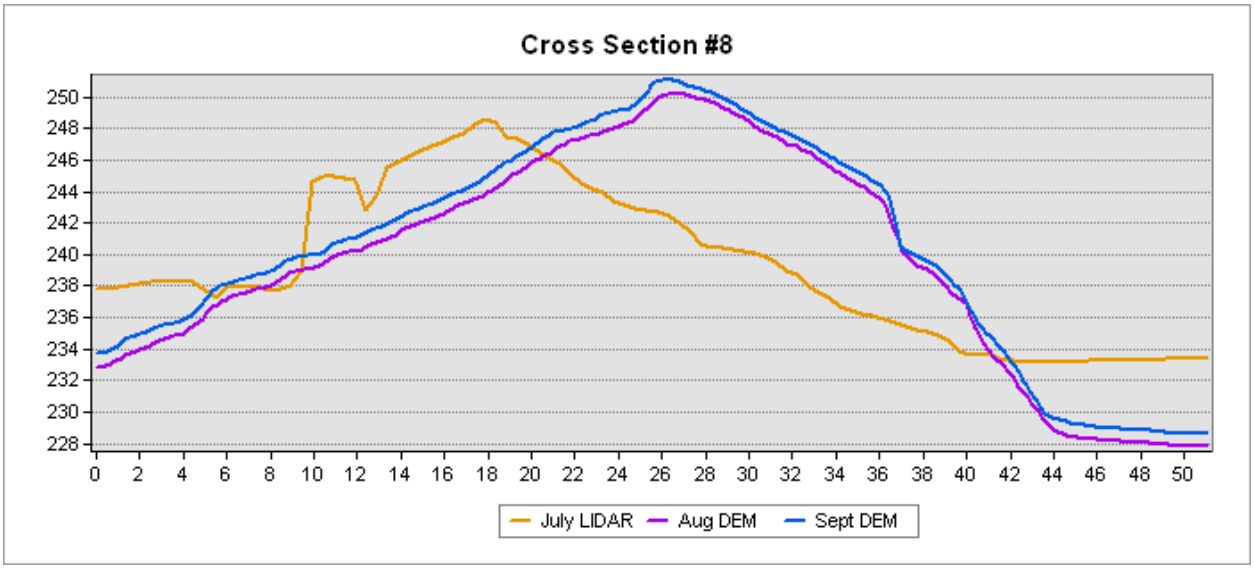
Cross Section #8
250
248
246
244
242
240
238
236
234
232
230
228
0
2
4
6
8
10
12
14
16
18
20
22
24
26
28
30
32
34
36
38
40
42
44
46
48
50
July LIDAR
Aug DEM
Sept DEM

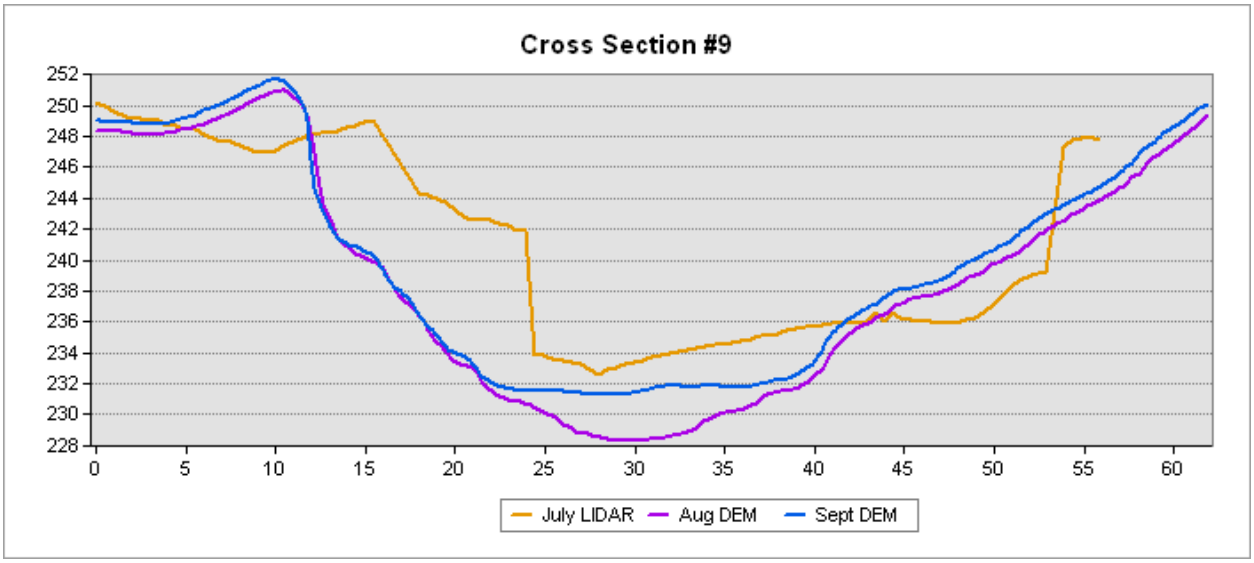
Cross Section #9
252
250
248
246
244
242
240
238
236
234
232
230
228
0
5
10
15
20
25
30
35
40
45
50
55
60
July LIDAR
Aug DEM
Sept DEM

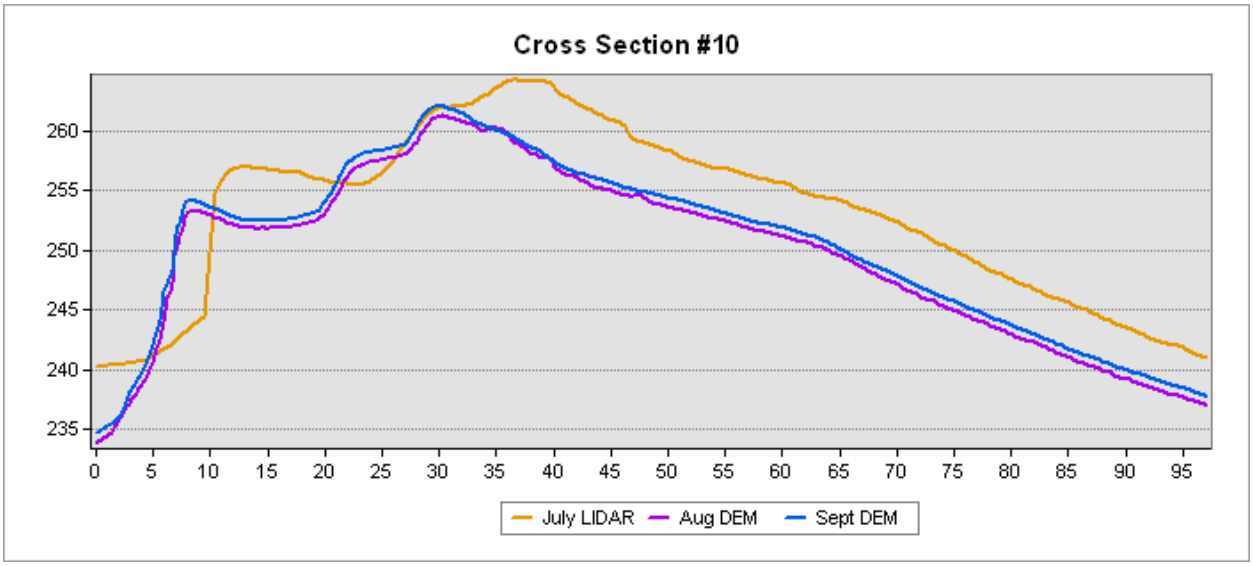
Cross Section #10
260
255
250
245
240
235
0
5
10
15
20
25
30
35
40
45
50
55
60
65
70
75
80
85
90
95
July LIDAR
Aug DEM
Sept DEM